Pergamon

Scripta Materialia, Vol. 38, No. 1, pp. 73–80, 1998
Elsevier Science Ltd

1359-6462/98 $19.00 + .00

PII S1359-6462(97)00409-0

MC CARBIDES IN THE Hf CONTAINING Ni BASED SUPERALLOY MarM002

M.J. Starink[1], H. Cama[2] and R.C. Thomson[1]
[1]Institute of Polymer Technology and Materials Engineering, Loughborough University, Loughborough LE11 3TU, UK
[2]Formerly Dept. of Materials Science and Metallurgy, University of Cambridge, Pembroke Street, Cambridge, UK, currently at Alcan International Ltd., Banbury Laboratory, Southam Road, Banbury, OX16 7SP, UK

(Received July 24, 1997)
(Accepted September 18, 1997)

Introduction

Conventionally cast nickel based superalloys, like the commercial alloy MarM002, are widely used in the manufacture of industrial gas turbine engine components which operate at elevated temperatures (700–900 °C) at medium to high stresses (200–350 MPa). These superalloys utilise two basic mechanisms for strengthening: solid solution strengthening, and precipitate strengthening through ordered intermetallic and carbide phases (1,2). The major phases present in nickel based superalloys include the austenitic γ matrix, carbides (MC, $M_{23}C_6$ and M_6C, where M stands for a combination of metallic elements), intermetallic phases such as γ', η (Ni_3Ti), ϵ (Ni_3Nb), borides (MB_2 and M_3B_2) and topologically closed packed (TCP) phases such as μ, σ and Laves phases (1,2). In order to utilise nickel based superalloys effectively, it is necessary to have a thorough understanding of the phases present and to establish the effect of exposure time and temperature on these phases.

This study focuses on the face centred cubic (NaCl structure) MC carbides in the conventionally cast MarM002 alloy. MC carbides are one of the most stable compounds in nature and consequently they form shortly after freezing in MarM002, just as they do in the similar MarM200 alloy (3) and other superalloys (1). Whilst in many commercial Ni based superalloys one type of MC carbide phase with a single well defined composition is thought to form, Ni based superalloys that contain Hf together with the common addition Ti generally contain two or more MC carbides with different compositions (3,4,5). Little information concerning the compositions of these different MC carbides has appeared in the open literature, and in this work we will present a detailed study of these carbides using X-ray diffraction (XRD), optical microscopy, scanning electron microscopy (SEM), transmission electron microscopy (TEM) and energy dispersive X-ray spectroscopy (EDX).

Experimental

Conventionally cast, uncoated MarM002 (nominal composition in mass %: 9% Cr, 10% W, 10% Co, 5.7% Al, 1.5% Ti, 2.5% Ta, 1.65% Hf, 0.06% Zr, 0.15% C, 0.013% B, bal Ni) blades were given a commercial heat treatment consisting of solutionising at 1190 °C for 15 minutes, followed by further

heat treatment at 870 °C for 18 hours. All samples were air cooled after each heat treatment. This condition will henceforth be referred to as the "unexposed" condition. Cylinders (5 mm diameter) were machined from the blades, and sealed in a quartz capsule under vacuum with a partial pressure of argon (20 kPa). Subsequent heat treatments were performed at 700, 800, 900 and 1000 °C for times up to 250 days and the samples were examined at 50 day intervals.

For optical microscopy, samples were mounted, ground, polished to a final finish of better than 0.25 μm and etched for 5 seconds in Kalling's reagent (40 g $CuCl_2$, 80 ml HCl and 40 ml methanol). SEM analysis was performed on a CAMSCAN 4 SEM operated at 20 kV. An energy dispersive X-ray (EDX) facility attached to the SEM was used for quantitative chemical analyses of the second phase particles within the blades. Corrections to account for effects due to atomic number (Z), absorption (A) and fluorescence (F) within the sample, were applied. A lifetime of 100 seconds was chosen to get good counting statistics.

To study the microstructure on a finer scale, single stage carbon extraction replicas were prepared and examined in a Philips 400T TEM operated at 120 kV. Samples made for optical microscopy were very lightly etched in Kalling's reagent and a uniform layer of carbon ($<$100 nm) was coated using a carbon arc source in a vacuum evaporation unit. The final extraction was performed using a simple electrolytic cell filled with 5% HCl in methanol and operated at 1.5 V. The replicas were collected from distilled water on to 200 mesh silver grids.

To extract particles, samples were immersed for 16 hours in an electrolytic cell (operated with 0.02 A) containing 10% HCl and 1% tartaric acid in methanol. These conditions are designed to dissolve the γ and γ' phase. The electrolytic cell was placed in an ultrasonic bath and the sample surface was periodically washed with methanol. Extracted particles were collected on an amorphous glass microfibre filter paper by filtration. The filter paper with the collected particles was examined in a Philips XPert diffractometer with a Cu X-ray tube at 40 kV and 40 mA. The samples were scanned over 2θ values ranging from 10–140 degrees. The widths of the divergence and receiving slits used were 1 and 0.1° respectively. Interplanar spacings used for peak identification were obtained from Powder Diffraction Files (PDF) cards.

Results

The microstructure of blades exposed at 700 and 800°C are similar to unexposed blades. All contain micrometer sized Chinese script-like and angular particles (see Fig. 1). These particles were observed to be uniformly distributed within the matrix. EDX analyses on the SEM revealed that both the Chinese script like and angular particles were rich in Hf, Ta, Ti and W which identifies them as face centred cubic (FCC) MC carbides (see e.g. Ref. 1). Selected area diffraction (SAD) in the TEM of several Hf-rich particles further confirmed this identification. Etching revealed dendritic contrast (Fig. 2). The dendritic regions show cuboid-like γ' (size about 0.5 μm) whilst interdendritic regions contain γ/γ' eutectic with larger, elongated primary γ' (Fig. 3). Further, much finer spherical γ' precipitates (diameter about 0.2 μm) are observed interspaced amongst both the primary γ' and the γ' in the dendrites. Apart from MC carbide, other finer carbide particles were also visible both within the γ/γ' eutectic and the dendritic regions. Cr-rich $M_{23}C_6$ was identified in both unexposed and exposed blades using SAD on the TEM.

Optical examination of unetched blades exposed for up to 250 days for all temperatures at 900 °C and 1000 °C again revealed micrometer sized Chinese script-like and angular MC carbides. With increasing exposure time and temperature, they appeared to coarsen up to a critical size and thereafter became finer/thinner and lost their distinct script like character. Etched samples after exposures for up to 250 days at 700–800 °C revealed dendritic contrast similar to that observed in the unexposed blade,

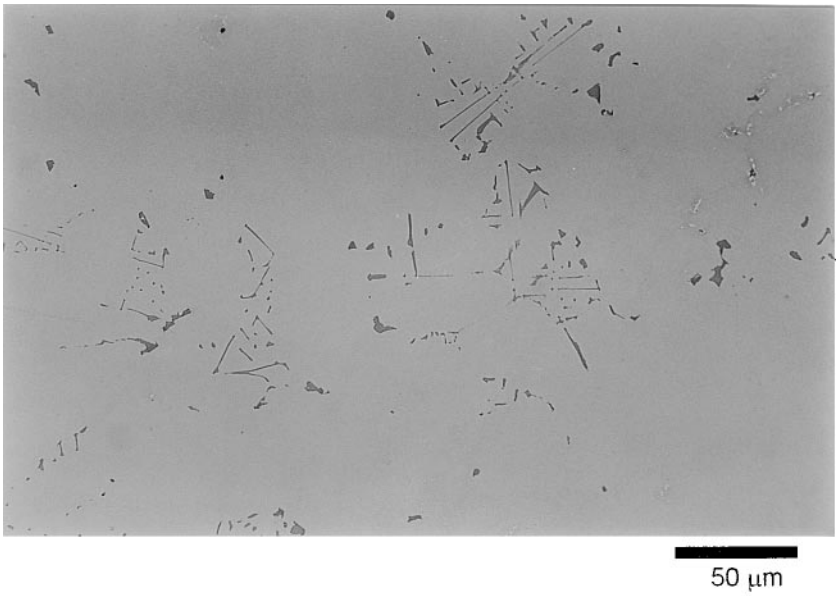

Figure 1. Optical micrograph of unexposed, unetched MarM002.

whilst at 900 and 1000 °C the dendritic contrast gradually diminishes. The interdendritic regions still contained γ/γ' eutectic.

The compositions of the MC carbides in the unexposed and exposed MarM002 samples were analysed in detail using EDX. All MC carbide particles contained significant amounts of Hf, Ta, Ti and W, whilst the occasional presence of other elements (Ni,Cr,Co) in the EDX analysis of especially the smaller particles was attributed to the matrix contribution to the signal. MC carbides with a wide range

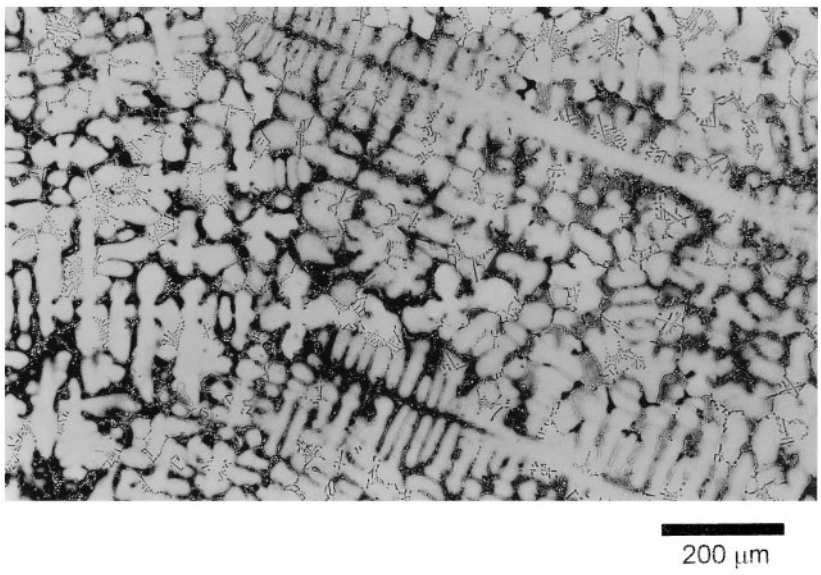

Figure 2. Optical micrograph of unexposed MarM002, etched to reveal dendritic contrast.

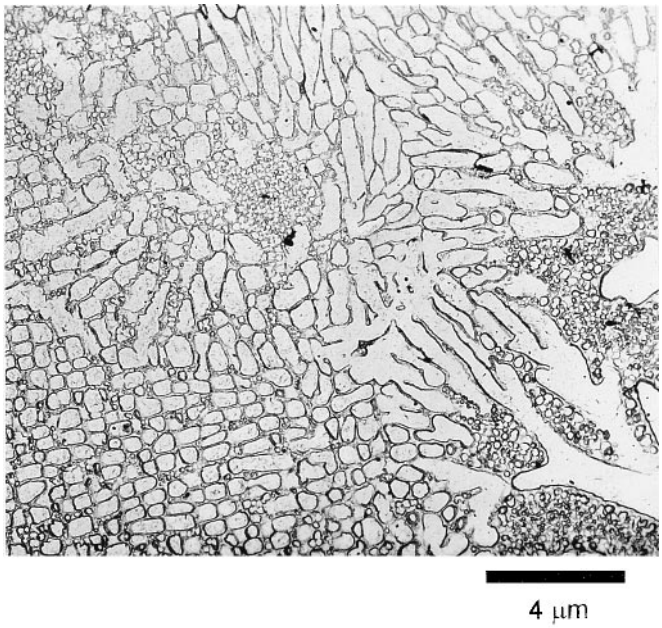

Figure 3. TEM micrograph of extraction replica of MarM002 exposed for 250 days at 700°C. The dendritic regions (bottom right) show cuboid like γ' whilst interdendritic regions contain γ/γ' eutectic with large elongated primary γ'. Through both regions much finer globular γ' is observed.

of compositions were observed and this range of compositions did not vary significantly with exposure at 700 and 800°C. The atomic fraction metallic elements, x_M, in the individual MC carbides after correction for matrix contributions is presented in Fig. 4. This figure shows that the compositions of MC carbides stretch from Hf-lean $(Ti_{0.4}Ta_{0.35}W_{0.2}Hf_{0.05})C$ to Hf rich $(Ti_{0.07}Ta_{0.12}W_{0.06}Hf_{0.75})C$. For lower

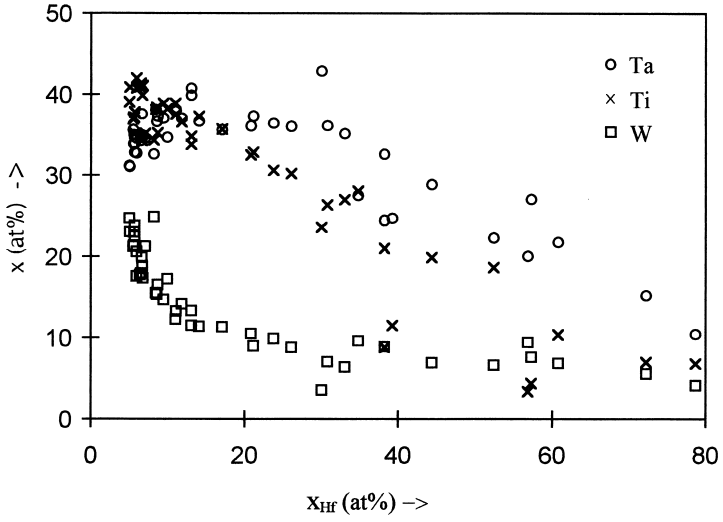

Figure 4. Compositions of individual MC carbides in unexposed MarM002 and MarM002 exposed at 700 and 800°C as measured by EDX.

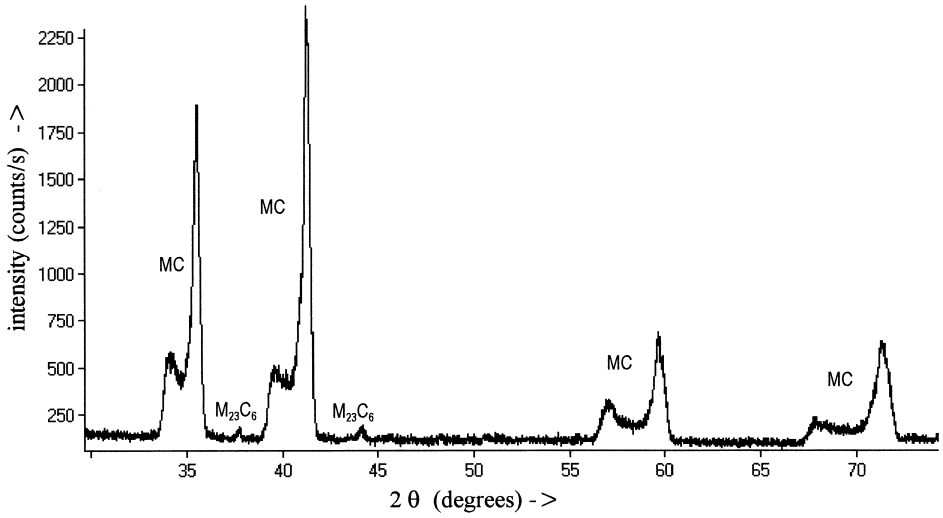

Figure 5. Part of the XRD spectrum of particles extracted from unexposed MarM002.

Hf contents ($x_{Hf} < 15$at%) Hf and W substitute for each other, whilst for intermediate Hf contents (15at% $< x_{Hf} <$ 60at%) the W content is constant and the Hf content increases by substituting Hf mainly for Ti. Analysis in the SEM shows that Hf-lean MC carbides are situated within the dendrites, whilst Hf rich carbides are situated on the core of the eutectic. In addition M in the MC carbides generally contains 3 to 6 at% Zr.

In Fig. 5 a part of the X-ray diffraction spectrum of unexposed MarM002 is presented. As expected no peaks due to γ or γ' phase are observed (they are dissolved during chemical extraction), and also peaks due to M_6C, borides (MB_2 or M_3B_2), μ or σ are absent. However, minor amounts of $M_{23}C_6$ were present as evidenced by small peaks (Fig. 5). As the other observed peaks fall within the range of positions of the cubic HfC, TaC, TiC and $Ti_{0.5}W_{0.5}C$ carbides, all other peaks are identified as due to MC carbides. The spectrum remains virtually unchanged during exposure at 700 and 800°C. After exposure at 900 and 1000 °C transformations occur in the types of carbides (see e.g. Refs. 2,4) which results in overlap with the complex MC carbide peaks, interfering with the analysis of the latter peaks. Hence, the analysis of the MC carbide peaks will be limited to unexposed samples and samples aged at 700°C and 800°C.

Discussion

To understand the X-ray diffraction patterns of the MC carbides it is first noted that at temperatures in excess of 1800°C ternary phase diagrams (6) indicate that the Hf, Ta and Ti in (Hf,Ta,Ti,W)C carbide are completely miscible, and significant amounts of W can dissolve in it. The ternary C-Ti-W diagram shows that (Ti,W)C is more stable than TiC as the former has a higher melting point. The maximum stability is at about $Ti_{0.5}W_{0.5}C$. Cubic WC is not a stable compound and instead the hexagonal WC appears in the equilibrium C-Ti-W diagram. Experimental work on the quasi-ternary TiC-HfC-WC system has shown the presence of a large miscibility gap with a ternary critical point at T_c=1800°C, $(TiC)_{0.55}(HfC)_{0.41}(WC)_{0.05}$ (7). In fact, also for other experimentally assessed quasi-ternary MC systems (for instance VC-HfC-WC, see Ref. 8) and for most quasi-binary systems (including HfC-TaC and HfC-TiC) miscibility gaps have either been proven or have been proposed to exist (6). The presence

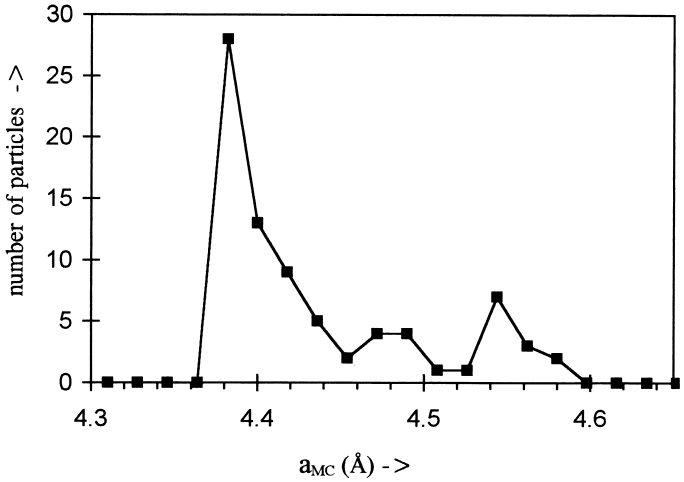

Figure 6. Frequency of the occurrence of MC carbides as a function of their lattice parameter as based on Eq. 1 and EDX data in Fig. 4.

of different MC carbides in Ti, Hf, W and Ta containing Ni-based superalloys (like the present MarM002) is related to the existence of such a miscibility gap in the TiC-HfC-WC-TaC system. During solidification this miscibility gap causes the formation of MC carbides with varying composition: at the start of solidification Hf-lean MC carbide forms, at intermediate stages of solidification MC carbides with intermediate Hf content form, whilst finally the Hf-rich variant forms in the eutectic. This view is consistent with the locations at which the carbides were detected (see previous section) and it is consistent with solidification studies of a similar MarM200 alloy (3).

Data on the lattice parameters of (Ti,Hf)C and (Hf,W)C (with $x_{Hf} < x_W$) shows that in these ternary carbides the influence of the metallic elements on the lattice parameter of the cubic MC carbide phase is in good approximation linear and additive (7). Assuming that this also holds for the (W,Hf,Ta,Ti)C phase, the lattice parameter can be calculated from the known lattice parameters, *a*, of HfC, TaC and TiC and the lattice parameter of the metastable cubic WC, i.e.:

$$a_{MC} = x_{HfC} + x_{Ti}\, a_{TiC} + x_{Ta}\, a_{TaC} + x_W\, a_{WC} + \delta a_{tern} \qquad (1)$$

where δa_{tern} is a (small) correction term to take ternary interactions resulting in deviations from linearity into account. Data on the HfC-TiC system (Hf and Ti are the main components in the MC phases studied) shows that δa_{tern} is very small (about 0.01 Å for $0.1 < x_{Hf}/x_{Ti} < 10$). In the HfC-WC system (see Ref. 7) the lattice parameter is a linear function of x_W for $x_W < 0.5$. (For $x_W > 0.5$ a negative deviation occurs.) In view of the compositions of the MC carbides in MarM002 (see Fig. 4), it can be estimated $\delta a_{tern} = 0.01$ Å. The lattice parameters of HfC, TiC and TaC are obtained from Ref. 9, whilst a_{WC} (4.33 Å) is estimated by extrapolating lattice parameter data in the HfC-WC system (see Ref. 7). Eq. 1 has been evaluated for the MC carbides using the EDX data on the compositions of the individual MC carbides (see Fig. 4), and the results (Fig. 6) are presented in the form of frequency distributions of the lattice parameters. In order to be able to construct the shape of a complex MC carbide diffraction peak from the data in Fig. 6 the following simplifying assumption is made: each carbide particle contributes to a complex of MC carbide peaks to a similar extent, i.e. no systematic dependency of MC particle size on composition exists. Results for the complex [220] peak are presented in Fig. 7. Comparison with Fig. 5 shows that within statistical error the present analysis can explain the shape and

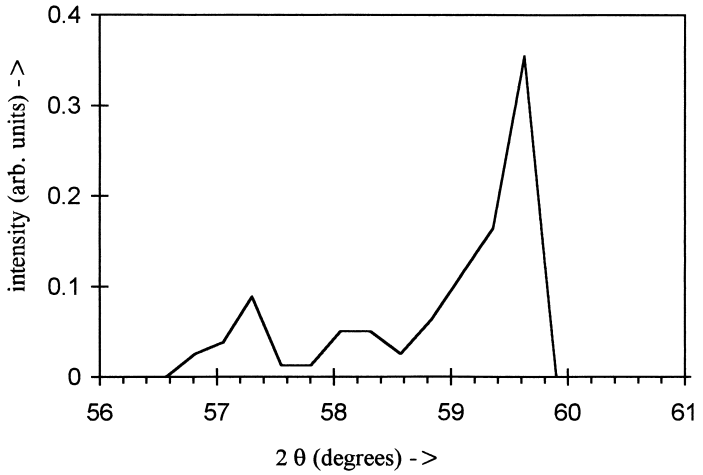

Figure 7. Calculated XRD spectrum based on Fig. 6.

position of the complex [220] peak quite well, and for the other complex peaks a similar correspondence can be obtained.

Work on the solidification of MarM002 and other Ni-based superalloys indicates that Ti rich MC can grow on Ti(C,N) (10,11). In correspondence with this minor peaks matching the pattern of the FCC (NaCl structure) Ti(C,N) phase were identified in XRD spectra of particles chemically extracted from some of the blades but were not detected as separate particles with TEM, SEM or EDX. This indicates that Ti(C,N) (or the structurally similar $Ti_{0.5}W_{0.5}C$ or BTi) exists as separate particles within the relatively large MC carbides. In a possible relation to the latter, the intensities of these minor peaks varied in a seemingly erratic manner between samples, which may reflect variations in the N (or B) content of the samples.

Although the lattice parameters and relative proportions of the various phases remain virtually unaltered during exposure at 700 and 800 °C, it is observed that similar exposures at higher temperatures 900-1000 °C result in increases in the relative proportions of Hf-rich MC, implying that the MC carbides are transforming to a more thermodynamically composition. It is noted that for all exposure temperatures, it is not the absolute value of the concentration of Hf that increases in the MC carbides with time, but it is the proportion of Hf-rich MC type carbides which increases in relation to the other MC phases.

Conclusions

Unexposed MarM002 alloy turbine blades and blades exposed at 700-1000°C for up to 250 days were studied by TEM, SEM, EDX and XRD. The shapes, distribution and compositions of the MC carbides do not vary significantly during exposure at 700 and 800°C. All MC carbides contain significant amounts of Hf, Ta, Ti and W, and they are present with a very broad range of compositions. The latter is caused by a miscibility gap in the MC carbide phase which causes the formation of MC carbides to shift from Hf lean in the initial stages of solidification to Hf rich in the later stages. In the unexposed samples the Hf lean (Ti,Ta)C carbide is the most numerous one. The shape of the complex MC carbide diffraction peaks are explained semi-quantitatively on the basis of the compositional range of the MC carbides.

Acknowledgements

The authors wish to thank Rolls Royce Industrial and Marine Gas Turbines Limited, Ansty, Coventry (UK) for providing funding for this project.

References

1. E. W. Ross and C. T. Sims, in Superalloys II, ed. C. T. Sims, N. S. Stofoff and W. C. Hagel, p. 97, John Wiley and Sons, New York (1987).
2. H. E. Collins and R. J. Quigg, Trans. ASM. 61, 139 (1968).
3. R. Sellamuthu and A. F. Giamei, Metall. Trans. 17A, 419 (1986).
4. H. E. Collins, Trans. ASM. 62, 82 (1968).
5. G. M. Janowski, B. S. Harmon, and B. J. Pletka, Metall. Trans. A. 18, 1341 (1987).
6. P. Villars, A. Prince, and H. Okamoto, ASM Handbook of Ternary Alloy Diagrams, ASM International, Metals Park, OH (1995).
7. P. Rogl, S. K. Naik, and E. Rudy, Mh. Chem. 108, 75 (1977).
8. P. Rogl, S. K. Naik, and E. Rudy, Mh. Chem. 108, 1213 (1977).
9. P. Villars and L. D. Calvert, Pearson's Handbook of Crystallographic Data for Intermetallic Phases, ASM, Metals Park, OH (1985).
10. G. L. R. Durber, S. Osgerby, and P. N. Quested, Metals Techn. 11, 129 (1984).
11. A. Mitchell, S. L. Cockcroft, C. E. Schvezov, A. J. Schmalz, J. N. Loquet, and J. Fernihough, High-Temp. Mater. and Processes. 15, 27 (1996).